Int J Ind Chem (2014) 5:19
DOI 10.1007/s40090-014-0019-3

RESEARCH

Corrosion inhibition effect and adsorption behaviour of nicotinamide derivatives on mild steel in hydrochloric acid solution

M. P. Chakravarthy · K. N. Mohana · C. B. Pradeep Kumar

Received: 15 February 2014 / Accepted: 12 July 2014 / Published online: 26 August 2014

Abstract

Background A new class of nicotinamide derivatives viz., *N*-((1H-pyrrol-2-yl)methylene)nicotinamide, *N*-((methyl-(phenyl)amino)methylene)nicotinamide, *N*-nicotinoylbenzimidothioic acid and *N*-(4-(methylthio)benzylidene)nicotinamide have been synthesized and their corrosion inhibition effect on mild steel in 0.5 M HCl was investigated by mass loss, Tafel polarization technique and AC impedance measurements.

Results The inhibition efficiency of the inhibitors on mild steel in 0.5 M HCl has been studied based on concentration, time interval and temperature. Potentiodynamic polarization studies showed that all the examined inhibitors suppress both anodic and cathodic process and behave as mixed type of corrosion inhibitors.

Conclusions The adsorption of all the inhibitors was found to obey Langmuir isotherm model. Electrochemical impedance data revealed that polarization resistance (R_P) increases and double layer capacitance (C_{dl}) decreases as the concentration of the inhibitors increases. FTIR, EDX and SEM analyses were performed to study the film persistency of the inhibitors.

Keywords Corrosion inhibition · Nicotinamide derivatives · Adsorption · Electrochemical techniques · Thermodynamic properties

M. P. Chakravarthy · K. N. Mohana (✉) · C. B. Pradeep Kumar
Department of Studies in Chemistry, University of Mysore, Manasagangothri, Mysore 570 006, India
e-mail: drknmohana@gmail.com

Background

Mild steel (MS) is a class of strong and tough steel that contains a low quantity of carbon. MS has relatively low tensile strength, but it is cheap and malleable, and its surface hardness can be increased through carburizing. It is the most important engineering material particularly for structural, instrumental, industrial and automobile applications. But it is highly susceptible to corrosion especially in acidic media [1]. Corrosion problem occurs in many industries, and can cause disastrous damage to metal and alloy structures causing economic consequences in terms of repair, replacement and product losses. Hence, various corrosion protection technologies have been employed, among them; the use of inhibitors is one of the practical methods for preventing corrosion of MS especially in acid media [2]. A wide variety of corrosion inhibitors ranging from rare earth elements [3] to organic compounds [4–7] have been used. The corrosion inhibition property of inhibitors depends on their molecular structures, planarity and the lone pairs of electrons present on the hetero atoms, which determine the adsorption of these molecules on the metallic surfaces. Corrosion inhibitors block the active sites and enhance the adsorption process, thus decreasing the rate of dissolution and extending the life span of the equipment [8, 9].

Although, several organic compounds have been used as inhibitors in different corrosive environment, choosing an appropriate inhibitor for specific environment and metal is of great importance. Generally, oxygen, nitrogen and sulphur containing heterocyclic organic compounds with multiple bonds have a tendency to resist corrosion [10, 11]. Compounds rich in heteroatoms can be regarded as environmental friendly inhibitors because of their characteristic strong chemical activity and low toxicity [12]. The

adsorption characteristics of organic molecules are also affected by sizes, electron density at the donor atoms and orbital character of donating electrons [13–16]. Organic compounds containing hetero atoms in the functional groups, pi-electron in triple or conjugated double bonds and presence of aromatic rings in their structure are the major adsorption centres and are usually good inhibitors [17]. Several heterocyclic compounds such as methylthiophenyl derivatives [18], isoxazolium cationic Schiff base compounds [19], quinoline derivatives [20], sulphonamide compounds [21], thiadiazoles derivatives [22], imidazole derivatives [23], fluoroquinolones [24], pyrazole derivatives [25], pyridazine derivatives [26] and pyridine derivatives [27] have been reported as anticorrosion substances in various corrosive environments.

In the present investigation attempts have been made to study the inhibitive effect of the four newly synthesized nicotinamide derivatives such as *N*-((1H-pyrrol-2-yl)methylene)nicotinamide (PMN), *N*-((methyl(phenyl)amino)-methylene)nicotinamide (MMN), *N*-nicotinoylbenzimidothioic acid (NBT) and *N*-(4-(methylthio)benzylidene)nicotinamide (MBN), on the corrosion of MS in 0.5 M HCl using mass loss and electrochemical techniques. The experimental results were discussed with various activation and adsorption thermodynamic parameters. The passive film formed on the metal surface was characterized by FTIR, SEM and EDX. Further, the inhibition performances of the four derivatives have been compared and discussed.

Experimental

Materials

MS specimen used in the present study having the following chemical compositions (in wt%): C 0.051; Mn 0.179; Si 0.006; P 0.005; S 0.023; Cr 0.051; Ni 0.05; Mo 0.013; Ti 0.004; Al 0.103; Cu 0.050; Sn 0.004; B 0.00105; Co 0.017; Nb 0.012; Pb 0.001 and the remainder iron. For all experiments, square type MS specimens of dimension 2 cm × 2 cm × 0.1 cm were used. The specimens were mechanically well polished with different grades SiC (200–600) emery papers, degreased with benzene, washed with doubly distilled water and finally dried. All solvents and chemicals used were of AR grade, and used as such. Doubly distilled water was used in the preparation of the various concentrations of test solutions.

Synthesis of inhibitors

The nicotinamide derivatives, PMN, MMN, NBT and MBN have been synthesized by the literature method [28].

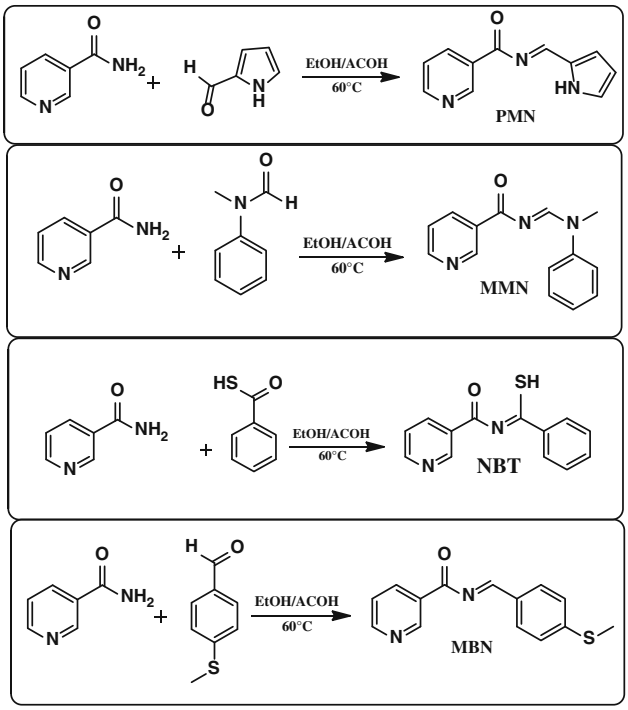

Fig. 1 Synthetic scheme of PMN, MMN, NBT and MBN

PMN was synthesized by dissolving 0.61 g (5 mmol) of nicotinamide ($C_6H_6N_2O$, Mol. Wt. 122.12) in 15 mL of ethanol in a round bottom flask. To this 0.47 g (5 mmol) of pyrrole-2-carboxaldehyde (C_5H_5NO, Mol. Wt. 95.10) in 15 mL ethanol was mixed and refluxed for 6 h at 60 °C temperature in the presence of few drops glacial acetic acid, and then the solution was concentrated using rotor vaporizer and kept for dry in vacuum. MMN was synthesized by dissolving 0.61 g (5 mmol) of nicotinamide in 15 mL of ethanol in a round bottom flask. To this 0.62 mL (5 mmol) of *N*-methylformanilide (C_8H_9NO, Mol. Wt. 135.16) in 15 mL ethanol was mixed and refluxed for 6 h at 60 °C temperature in the presence of few drops glacial acetic acid, and then the solution was concentrated using rotor vaporizer and kept for dry in vacuum.

NBT was synthesized by dissolving 0.61 g (5 mmol) of nicotinamide in 15 mL of ethanol in a round bottom flask. To this 0.58 mL (5 mmol) of thiobenzoic acid (C_7H_6OS, Mol. Wt. 138.19) dissolved in 15 mL of ethanol was added and refluxed for 6 h with stirring at 60 °C temperature in the presence of few drops of glacial acetic acid. Then the solution was concentrated using rotor vaporizer and kept for dry in vacuum and the product obtained was collected. MBN was synthesized by dissolving 0.61 g (5 mmol) of nicotinamide in 15 mL of ethanol in a round bottom flask. To this a 0.66 mL (5 mmol) of the 4-(methylthio)benzaldehyde (C_8H_8OS, Mol. Wt. 152.21) dissolved in 15 mL of ethanol was added and refluxed for 6 h with stirring at

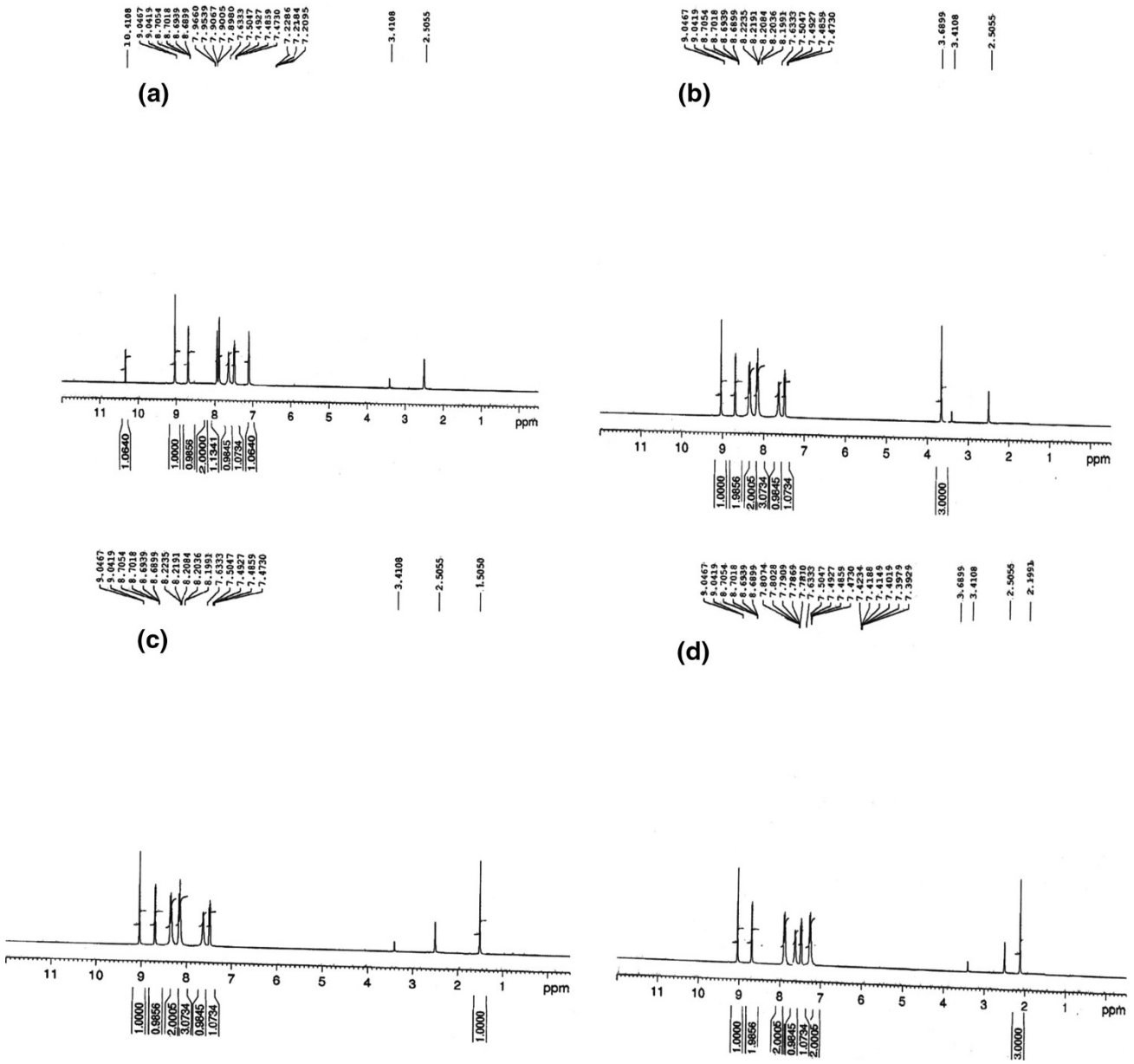

Fig. 2 ^{1}H-NMR spectrum of **a** PMN, **b** MMN, **c** NBT and **d** MBN

60 °C temperature in presence of glacial acetic acid. Then the solution was concentrated using rotor vaporizer and kept for dry in vacuum and the product obtained was collected. The synthetic schemes of PMN, MMN, NBT and MBN are shown in Fig. 1.

The Chemical structures of the compounds are characterized by FTIR, ^{1}H-NMR and Mass spectral studies. PMN ($C_{11}H_9N_3O$, Mol. Wt. 199.21): Yield: 89 %, Melting Range (M. R, °C): 98–102. FTIR (KBr, cm^{-1}): 1,457 (NH), 1,645 (N=C), 1,726 (C=O). ^{1}H-NMR (400.15 MHz, DMSO-d6) δ ppm: 7.22–7.20 (t, $J = 4.0$ Hz, 1H), 7.50–7.47 (q, 1H), 7.63 (s, 1H), 7.90–7.89 (t, $J = 4.2$ Hz, 1H), 7.96–7.95 (d, $J = 4.8$ Hz, 2H), 8.70–8.68 (t, $J = 3.8$ Hz, 1H), 9.046–9.041 (d, $J = 2.0$ Hz, 1H), 10.41 (s, 1H). MS, *m/z*: 200 (M+1). Elemental analyses found (calculated) for $C_{11}H_9N_3O$ (%): C, 66.29 (66.32): H, 4.50 (4.55): N, 20.96 (21.09), O, 7.98 (8.03). ^{1}H-NMR spectrum of PMN is shown in Fig. 2a.

MMN ($C_{14}H_{13}N_3O$, Mol. Wt. 239.27): Yield: 79 %, Melting Range (M. R, °C): 106–108. FTIR (KBr, cm^{-1}): 1,630 (N=C), 1,710 (C=O). ^{1}H-NMR (400.15 MHz, DMSO-d6) δ ppm: 3.68 (s, 3H), 7.50–7.47 (q, 1H), 7.63 (s, 1H), 8.20–8.19 (d, $J = 1.8$ Hz, 3H), 8.22–8.20 (t, $J = 4.0$ Hz, 2H), 8.70–8.68 (q, 2H), 9.046–9.041

Table 1 C_R and IE (%) obtained from mass loss measurements of MS in 0.5 M HCl solution containing various concentrations of PMN, MMN, NBT and MBN at different temperatures

T (°C)	C (ppm)	PMN		MMN		NBT		MBN	
		C_R (mg cm^{-2} h^{-1})	IE (%)	C_R (mg cm^{-2} h^{-1})	IE (%)	C_R (mg cm^{-2} h^{-1})	IE (%)	C_R (mg cm^{-2} h^{-1})	IE (%)
30	Blank	0.7200	–	0.7200	–	0.7200	–	0.7200	–
	200	0.2324	67.6	0.1979	72.6	0.1582	78.1	0.1340	81.4
	300	0.1875	74.0	0.1520	78.9	0.1307	81.9	0.0987	86.3
	400	0.1715	76.2	0.1288	82.1	0.1074	85.1	0.0718	90.0
	500	0.1400	80.6	0.0984	86.3	0.0811	88.7	0.0464	93.6
40	Blank	0.9490	–	0.9490	–	0.9490	–	0.9490	–
	200	0.3202	66.2	0.2711	71.4	0.2180	77.0	0.1878	80.2
	300	0.2814	70.3	0.2315	75.6	0.1959	79.3	0.1514	84.0
	400	0.2381	74.9	0.1879	80.2	0.1611	83.0	0.1109	88.3
	500	0.2049	78.4	0.1500	84.2	0.1207	87.3	0.0786	91.7
50	Blank	1.1520	–	1.1520	–	1.1520	–	1.1520	–
	200	0.4090	64.5	0.3557	69.1	0.2846	75.3	0.2491	78.4
	300	0.3562	69.1	0.2994	74.0	0.2532	78.0	0.1928	83.3
	400	0.3142	72.7	0.2473	78.5	0.2206	80.8	0.1670	85.5
	500	0.2676	76.8	0.2036	82.3	0.1645	85.7	0.1112	90.3
60	Blank	1.4350	–	1.4350	–	1.4350	–	1.4350	–
	200	0.5376	62.5	0.4687	67.3	0.3895	72.9	0.3551	75.3
	300	0.4555	68.3	0.3864	73.1	0.3277	77.2	0.2552	82.2
	400	0.4235	70.5	0.3502	75.6	0.2871	80.0	0.2248	84.3
	500	0.3606	74.9	0.2730	81.0	0.2293	84.0	0.1764	87.7

(d, $J = 2.0$ Hz, 1H). MS, *m/z*: 240 (M+1). Elemental analyses found (calculated) for $C_{14}H_{13}N_3O$ (%): C, 70.19 (70.28): H, 5.41 (5.48): N, 17.48 (17.56), O, 6.57 (6.69). ^{1}H-NMR spectrum of MMN is shown in Fig. 2b.

NBT ($C_{13}H_{10}N_2OS$, Mol. Wt. 242.30): Yield: 83 %, Melting Range (M. R, °C): 82–84. FTIR (KBr, cm^{-1}): 723 (C–S), 1,643 (N=C), 1,726 (C=O). ^{1}H-NMR (400.15 MHz, DMSO-d6) δ ppm: 1.50 (s, 1H), 7.50–7.47 (q, 1H), 7.63 (s, 1H), 8.20–8.19 (d, $J = 1.8$ Hz, 3H), 8.22–8.20 (t, $J = 4.2$ Hz, 2H), 8.70–8.68 (q, 1H), 9.046–9.041 (d, $J = 2.0$ Hz, 1H). MS, *m/z*: 243 (M+1). Elemental analyses found (calculated) for $C_{13}H_{10}N_2OS$ (%): C, 64.38 (64.44): H, 4.07 (4.16): N, 11.44 (11.56), O, 6.58 (6.60), S, 13.17 (13.23). ^{1}H-NMR spectrum of NBT is shown in Fig. 2c.

MBN ($C_{14}H_{12}N_2OS$, Mol. Wt. 256.32): Yield: 85 %, Melting Range (M. R, °C): 90–94. FTIR (KBr, cm^{-1}): 667 (C–S), 1,587 (N=C), 1,697 (C=O). ^{1}H-NMR (400.15 MHz, DMSO-d6) δ ppm: 2.19 (s, 3H), 7.42–7.39 (m, 2H), 7.50–7.47 (q, 1H), 7.63 (s, 1H), 7.80–7.78 (m, 2H), 8.70–8.68 (q, 2H), 9.046–9.041 (d, $J = 2.0$ Hz, 1H). MS, *m/z*: 257 (M+1). Elemental analyses found (calculated) for $C_{14}H_{12}N_2OS$ (%): C, 65.54 (65.60): H, 4.68 (4.72): N, 10.89 (10.93), O, 6.19 (6.24), S, 12.47 (12.51). ^{1}H-NMR spectrum of MBN is shown in Fig. 2d.

Methods

Mass loss measurements

Mass loss measurements were performed by weighing cleaned and dried MS specimens before and after immersion in 0.5 M HCl solutions from 1 to 5 h in the absence and presence of various concentrations of PMN, MMN, NBT and MBN at different temperatures (30–60 °C). Triplicate experiments were performed in each case and the mean value of the mass loss was noted. Corrosion rate (C_R) in mg cm^{-2} h^{-1} and inhibition efficiency IE (%) were calculated using the following equations:

$$C_R = \frac{\Delta M}{St} \quad (1)$$

where ΔM is the mass loss, S is the surface area of the specimen and t is the immersion time.

$$\text{IE}\,(\%) = \frac{(C_R)_a - (C_R)_p}{(C_R)_a} \times 100 \quad (2)$$

where $(C_R)_a$ and $(C_R)_p$ are the corrosion rates in the absence and presence of inhibitor, respectively.

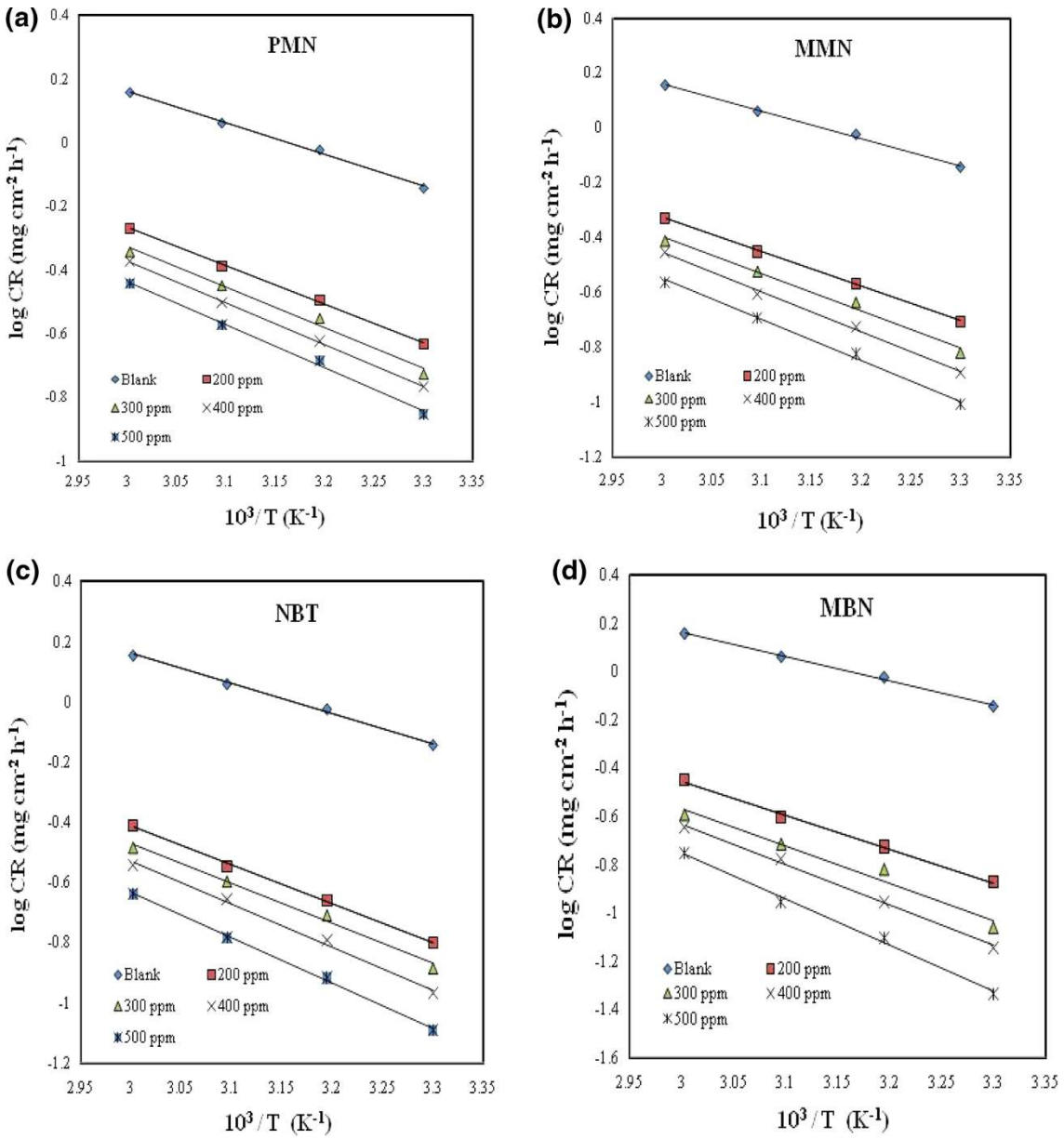

Fig. 3 Plot of log C_R versus $1/T$ for **a** PMN, **b** MMN, **c** NBT and **d** MBN

Potentiodynamic polarization measurements

The potentiodynamic polarization studies were carried out with MS specimen as working electrode in 0.5 M HCl solutions with different inhibitor's concentrations (200–500 ppm) with an exposed area of 1 cm^2 and this working area was remained precisely fixed throughout the experiment. A conventional three electrode cell consisting of MS as working electrode, platinum foil as counter electrode and saturated calomel electrode (SCE) as reference electrode was used. Potentiodynamic polarization studies were carried out using CH-instrument (model CHI660D). Before each Tafel experiment, the MS electrode was allowed to corrode freely and its open circuit potential (OCP) was recorded as a function of time up to 30 min. After this time, a steady state OCP corresponding to the corrosion potential (E_{corr}) of the working electrode was obtained. The IE (%) was calculated from corrosion currents determined from the Tafel extrapolation plot method using the experimental relation:

$$\text{IE } (\%) = \frac{(I_{corr})_a - (I_{corr})_p}{(I_{corr})_a} \times 100 \quad (3)$$

where $(I_{corr})_a$ and $(I_{corr})_p$ are the corrosion current density ($\mu A\ cm^{-2}$) in the absence and presence of the inhibitor, respectively.

Table 2 Values of activation parameters for MS in 0.5 M HCl medium in the absence and presence of various concentrations of PMN, MMN, NBT and MBN

Inhibitor	C (ppm)	E_a (kJ mol^{-1})	ΔH_a (kJ mol^{-1})	$\Delta H_a = E_a - RT$ (kJ mol^{-1})	ΔS_a (J mol^{-1} K^{-1})
Blank	0	19.0	16.4	16.5	−197.6
PMN	200	23.2	20.5	20.6	−189.4
	300	24.4	21.7	21.8	−186.9
	400	25.0	22.4	22.5	−185.7
	500	26.0	23.3	23.5	−184.1
MMN	200	24.0	21.3	21.5	−188.0
	300	25.7	23.0	23.1	−184.3
	400	27.5	24.8	24.9	−180.1
	500	28.3	25.6	25.8	−179.5
NBT	200	24.9	22.2	22.4	−187.0
	300	25.3	22.7	22.8	−186.8
	400	27.4	24.8	24.9	−181.6
	500	28.8	26.1	26.2	−179.6
MBN	200	26.9	24.2	24.3	−181.9
	300	29.3	26.6	26.8	−176.8
	400	32.2	29.5	29.7	−169.3
	500	36.5	33.9	34.0	−158.6

Electrochemical impedance spectroscopy (EIS)

Electrochemical impedance spectroscopy measurements were carried out using the same CH-instrument. The EIS data were taken in the frequency range 10–0.05 kHz. The double layer capacitance (C_{dl}) and the polarization resistance (R_p) were determined from Nyquist plots [29]. The percentage inhibition efficiency, IE (%) was calculated from R_p values using the following expression:

$$\text{IE } (\%) = \frac{1/(R_p)_a - 1/(R_p)_p}{1/(R_p)_a} \times 100 \quad (4)$$

where $(R_p)_a$ and $(R_p)_p$ are polarization resistances in the absence and presence of inhibitor, respectively.

FTIR, EDX and SEM studies

The MS specimens were immersed in 0.5 M HCl in the presence of inhibitors (500 ppm) for a period of 1 h. Then the specimens were taken out and dried. The surface adhered film was scratched carefully and its FTIR spectra were recorded using a Jasco FTIR 4100 double beam spectrophotometer. The surface feature of the MS specimens in the absence and presence of inhibitors was studied by energy dispersive X-ray spectroscopy (EDX) and scanning electron microscope (model JSM-5800).

Characterization of inhibitors

Melting range was determined by Veego Melting Point VMP III apparatus. FTIR spectra were recorded using a Jasco FTIR 4100 double beam spectrophotometer. ^{1}H-NMR spectra were recorded on Bruker DRX-500 spectrometer at 400 MHz using DMSO-d_6 as solvent and TMS as an internal standard. Mass spectral data were obtained by LC/MSD Trap XCT. Elemental analyses were recorded on VarioMICRO superuser V1.3.2 Elementar.

Results and discussion

Mass loss studies

The C_R and IE (%) in the absence and presence of various concentrations of PMN, MMN, NBT and MBN in 0.5 M HCl solution and at different temperatures (30–60 °C) are presented in Table 1. The mass loss was found to be decreased and IE (%) observed to be increased with increase in concentration of nicotinamide derivatives. The studied inhibitors were found to attain the maximum inhibition efficiency at 500 ppm. Further increase in concentration (beyond 500 ppm) did not cause any remarkable change in the inhibition efficiency. This conclusion is also supported by electrochemical studies. There is no appreciable increase in the inhibition efficiency after 1 h of immersion time, this is due to desorption of the inhibitor molecules from the metal surface with increasing immersion time and instability of the inhibitor film on the metal surface [30, 31]. The IE (%) of nicotinamide derivatives follows the order: MBN > NBT > MMN > PMN. The inhibition efficiency obtained from weight loss measurements is lower than that for electrochemical experiments, this phenomenon attributed to the fact that the weight loss

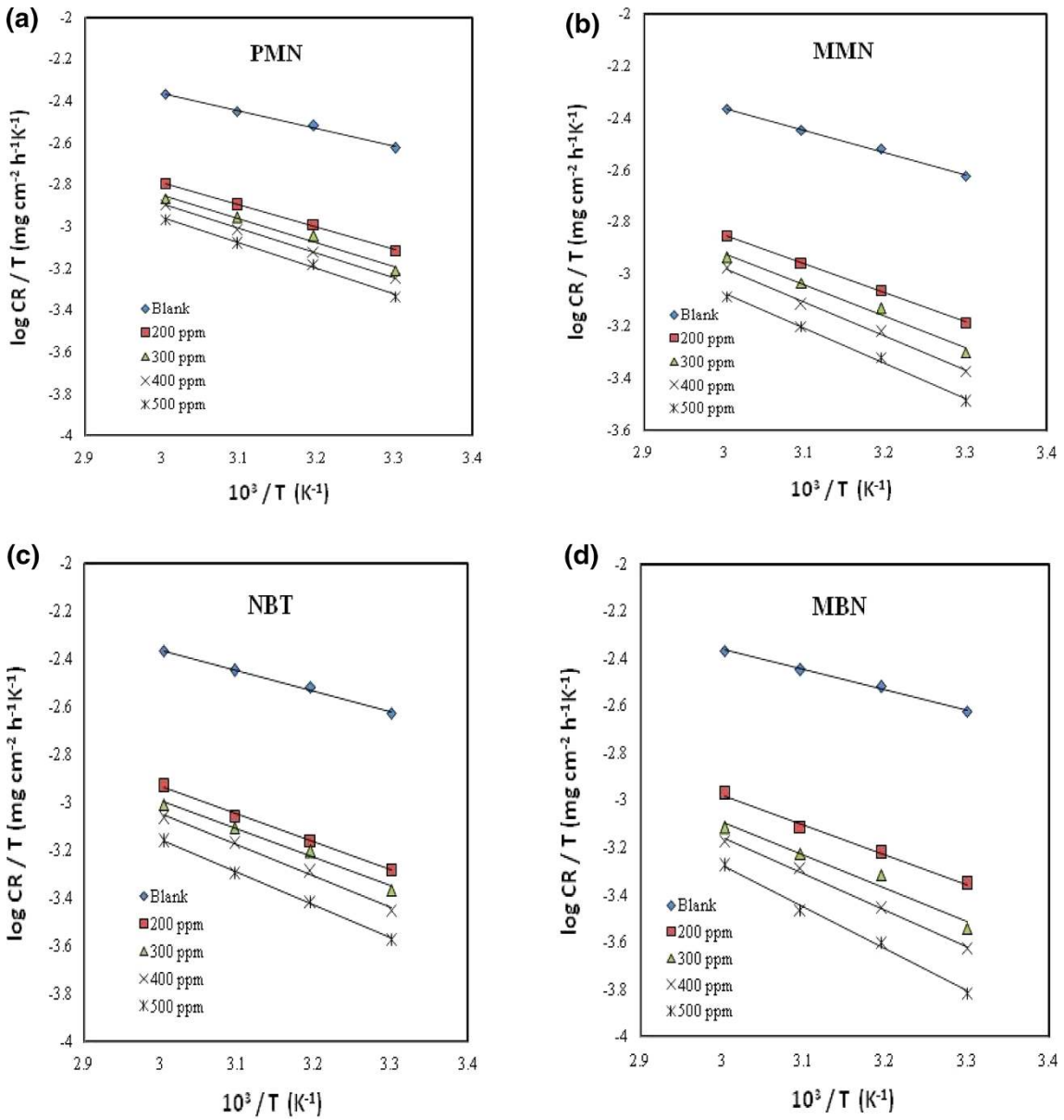

Fig. 4 Alternative Arrhenius plots for MS dissolution in 0.5 M HCl medium in the absence and presence of **a** PMN, **b** MMN, **c** NBT and **d** MBN

experiment gives average corrosion rates whereas the electrochemical experiments give instantaneous corrosion rates.

Effect of temperature

The effect of temperature on C_R and IE (%) was studied in 0.5 M HCl in the temperature range of 30–60 °C in the absence and presence of different concentrations of inhibitors (Table 1). The inhibition efficiencies were found to decrease with increasing temperature from 30 to 60 °C.

This may be explained with desorption of adsorbed inhibitor molecules on the MS surface. This proves that the inhibition occurs through the adsorption of the inhibitors on the metal surface, and desorption is aided by increasing temperature. The activation parameters for the corrosion process were calculated from the Arrhenius type plot according to the following equation:

$$C_R = k\exp^{-E_a/RT} \quad (5)$$

where E_a is the activation energy, k is the frequency factor, T is the absolute temperature and R is the universal gas constant. The values of E_a for MS in 0.5 M HCl without

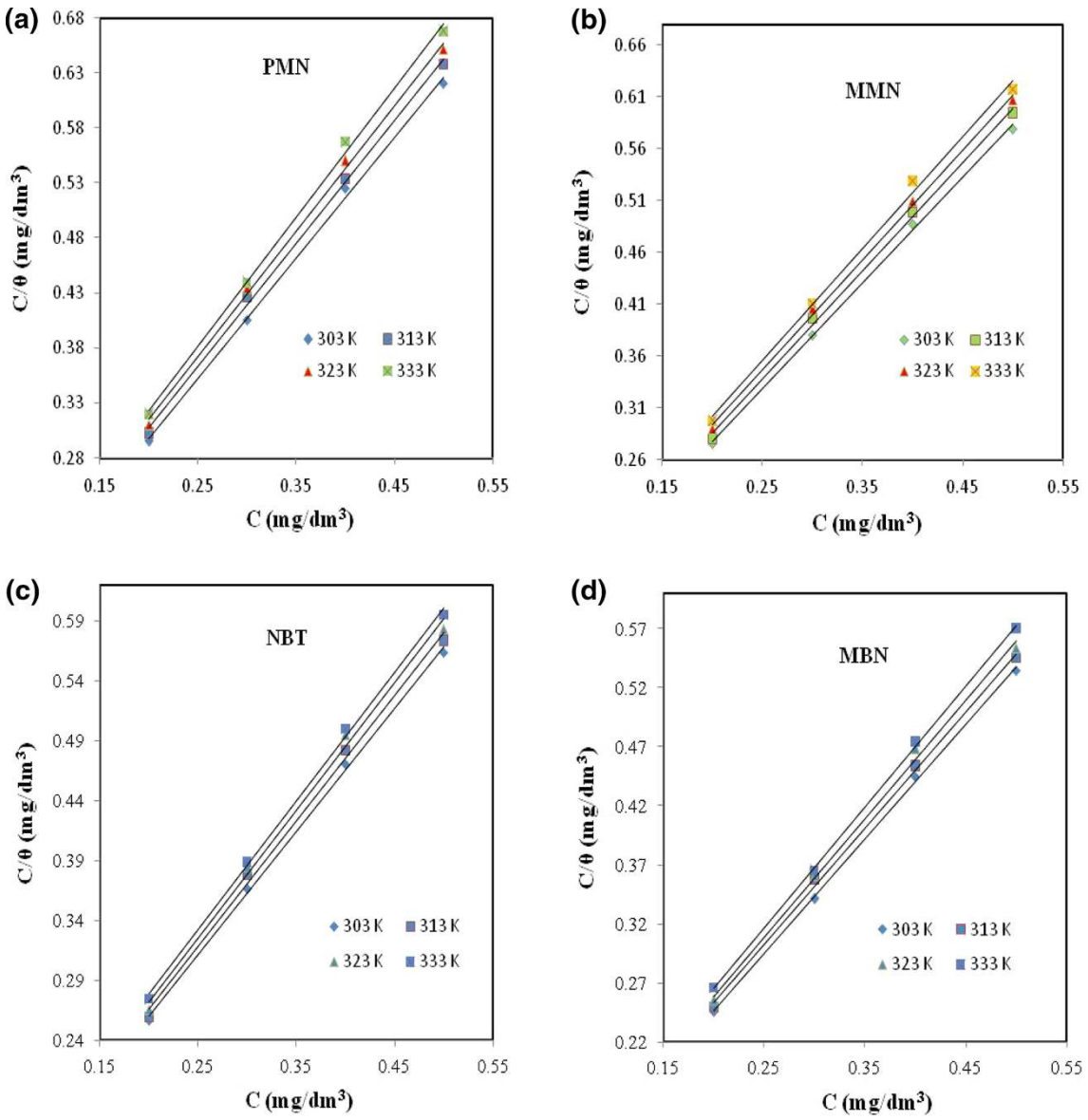

Fig. 5 Langmuir's adsorption isotherm plots for the adsorption of **a** PMN, **b** MMN, **c** NBT and **d** MBN in 0.5 M HCl on MS surface at different temperature

and with various concentrations of inhibitors were obtained from the slope of the plot of log C_R versus $1/T$ (Fig. 3) and are shown in Table 2. It was found that E_a values for inhibited systems are higher than those for the uninhibited systems (Table 2). This increase in the activation energy decreases the corrosion rate of metal [32]. With increasing temperature there is an appreciable decrease in the adsorption of the inhibitors on the metal surface and a corresponding rise in the corrosion rate occurred.

An alternative Arrhenius plots of log C_R/T versus $1/T$ (Fig. 4) for MS dissolution in 0.5 M HCl medium in the absence and presence of different concentrations of PMN, MMN, NBT and MBN were used to calculate the values of activation thermodynamic parameters such as enthalpy of activation (ΔH_a) and entropy of activation (ΔS_a) using the relation (6),

$$C_R = \frac{RT}{Nh}\exp\left(\frac{\Delta S_a}{R}\right)\exp\left(\frac{-\Delta H_a}{RT}\right) \quad (6)$$

where R is the universal gas constant, T is the absolute temperature, N is the Avogadro's number, h is Planks constant. The values of ΔH_a and ΔS_a were obtained from the slope and intercept of the above plot, and presented in Table 2. The obtained ΔH_a values are in good agreement with the calculated ΔH_a from the equation, $\Delta H_a = E_a - RT$.

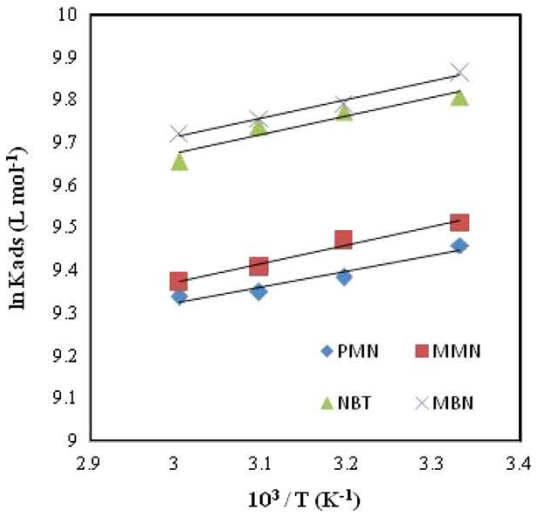

Fig. 6 Plot of $\ln K_{ads}$ versus $1/T$ for PMN, MMN, NBT and MBN

The positive values of enthalpy of activation in the absence and presence of inhibitors indicate an endothermic nature of MS dissolution process [33], and increase in the entropy of activation values decreases in the system disorder due to the adsorption of inhibitor molecules on the MS surface [34–36].

Adsorption isotherm

The efficiency of a corrosion inhibitor mainly depends on its adsorption ability on the metal surface. So, it is necessary to know the mechanism of adsorption and the adsorption isotherm that can give valuable information on the interaction of inhibitor and metal surface. The adsorption of inhibitor molecules from aqueous solution is a quasi-substitution process, and was found to be highly pH dependent [37]. The surface protection of MS depends upon how the inhibitor molecule will adsorbed on the metal surface, and also ionization and polarization of molecule [38]. The degree of surface coverage (θ) as function of concentration (C) of the inhibitor was studied graphically by fitting it to various adsorption isotherms to find the best adsorption isotherm. The Langmuir adsorption isotherm model was taken into account since equilibrium adsorption of all the four inhibitors was found to obey this adsorption isotherm model on MS in 0.5 M HCl medium. According to this adsorption isotherm, θ is related to the inhibitor concentration, C and adsorption equilibrium constant K_{ads} through the following expression:

$$C/\theta = \frac{1}{K_{ads}} + C \tag{7}$$

The surface coverage was tested graphically for fitting a suitable adsorption isotherm. In the present case, the plots of C/θ versus C (Fig. 5) yield straight lines with the linear correlation coefficient (R^2) values close to unity, which suggests that the adsorption of PMN, MMN, NBT and MBN in 0.5 M HCl medium on MS surface obeys the Langmuir adsorption isotherm. The Gibbs free energy of adsorption was calculated using the relation (8):

$$\Delta G^{\circ}_{ads} = -2.303RT \log 55.5K_{ads} \tag{8}$$

where R is the universal gas constant, T is the absolute temperature, K_{ads} is the equilibrium constant for adsorption–desorption process and 55.5 is the molar concentration

Table 3 Thermodynamic parameters for adsorption of PMN, MMN, NBT and MBN on MS in 0.5 M HCl at different temperatures

Inhibitor	T (°C)	R^2	K_{ads} (L mol^{-1})	ΔG°_{ads} (kJ mol^{-1})	ΔH°_{ads} (kJ mol^{-1})	ΔS°_{ads} (J mol^{-1} K^{-1})
PMN	30	0.998	12,820	−33.95		
	40	0.998	11,904	−34.87	0.376	8.95
	50	0.998	11,494	−35.89		
	60	0.997	11,363	−36.97		
MMN	30	0.999	13,513	−34.08		
	40	0.997	12,987	−35.10	0.438	8.056
	50	0.998	12,195	−36.05		
	60	0.996	11,764	−37.07		
NBT	30	0.998	18,181	−34.83		
	40	0.996	17,543	−35.88	0.442	8.348
	50	0.995	16,949	−36.94		
	60	0.998	15,625	−37.86		
MBN	30	0.999	19,230	−34.97		
	40	0.998	17,857	−35.93	0.434	8.411
	50	0.997	17,241	−36.98		
	60	0.999	16,666	−38.04		

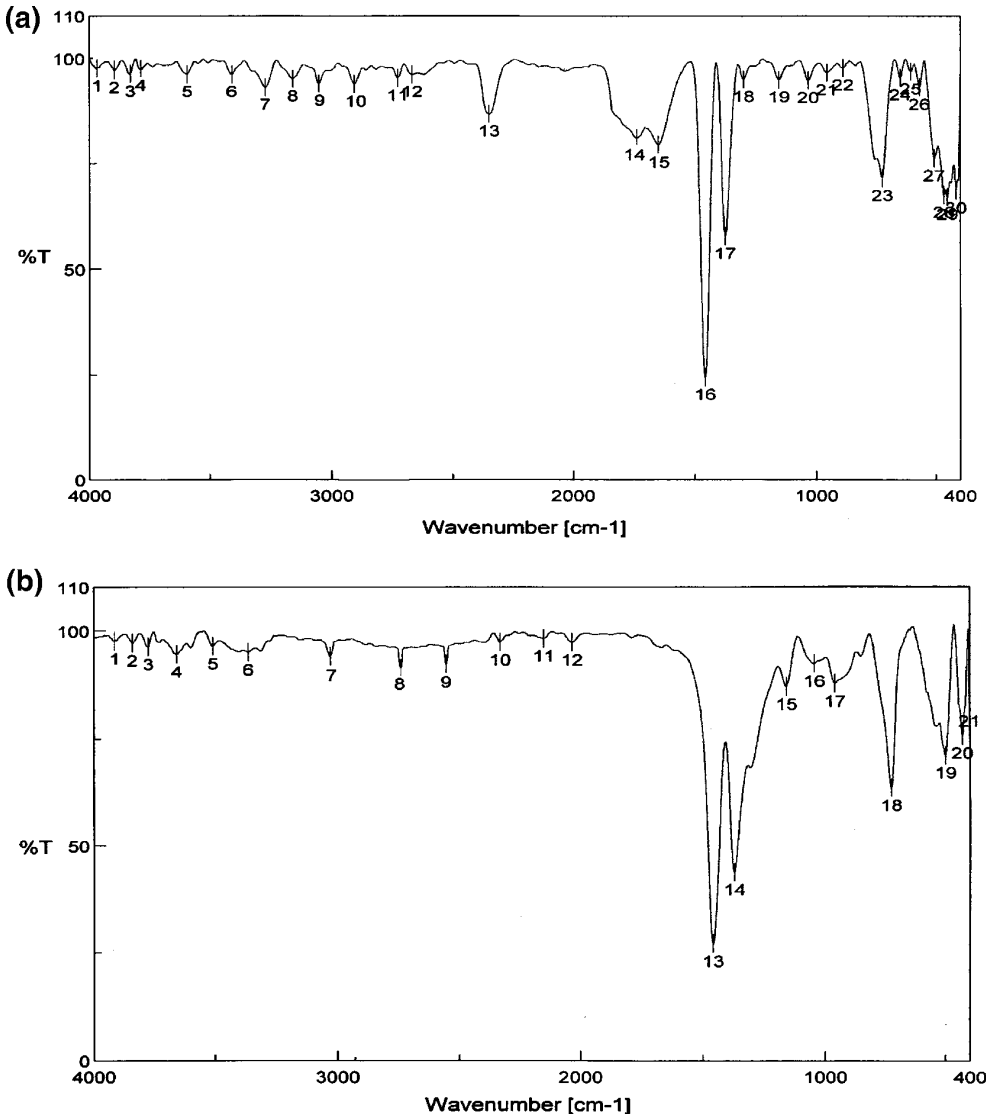

Fig. 7 FTIR spectra of **a** PMN and **b** scratched MS surface adsorbed PMN film

of water in solution (mol L^{-1}). The other adsorption thermodynamic parameters such as enthalpy of adsorption (ΔH°_{ads}) and entropy of adsorption (ΔS°_{ads}) were obtained from the slope and intercept of the plot of log K_{ads} versus $1/T$ (Fig. 6) using the Eq. (9).

$$\log K_{ads} = \frac{1}{2.303}\left(-\frac{\Delta H^{\circ}_{ads}}{RT}\right) + \left(\frac{\Delta S^{\circ}_{ads}}{R}\right) \quad (9)$$

The calculated values of K_{ads}, ΔH°_{ads}, ΔG°_{ads} and ΔS°_{ads} over the temperature range of 30–60 °C are recorded in Table 3. The negative values of ΔG°_{ads} indicate the spontaneous adsorption of inhibitors on the surface of MS [39]. In the present study, ΔG°_{ads} values for PMN, MMN, NBT and MBN are found to be in the range −33.95 to −36.97, −34.08 to −37.07, −34.83 to −37.86 and −34.97 to −38.04 kJ mol^{-1} in the temperature range of 30–60 °C, respectively indicating that the adsorption is the combination of both physisorption and chemisorption [40–43].

FTIR spectral studies

FTIR spectra were recorded to understand the interaction of inhibitor molecules with the metal surface. Figures 7a, 8a, 9a and 10a show the FTIR spectra of pure PMN, MMN, NBT and MBN, and Figs. 7b, 8b, 9b and 10b represent the FTIR spectra of the scrapped samples obtained from the metal surfaces after corrosion experiments. It was found that peaks in the spectrum of scrapped samples were changed when compared to pure compounds. The azomethine group stretching frequencies for pure PMN, MMN,

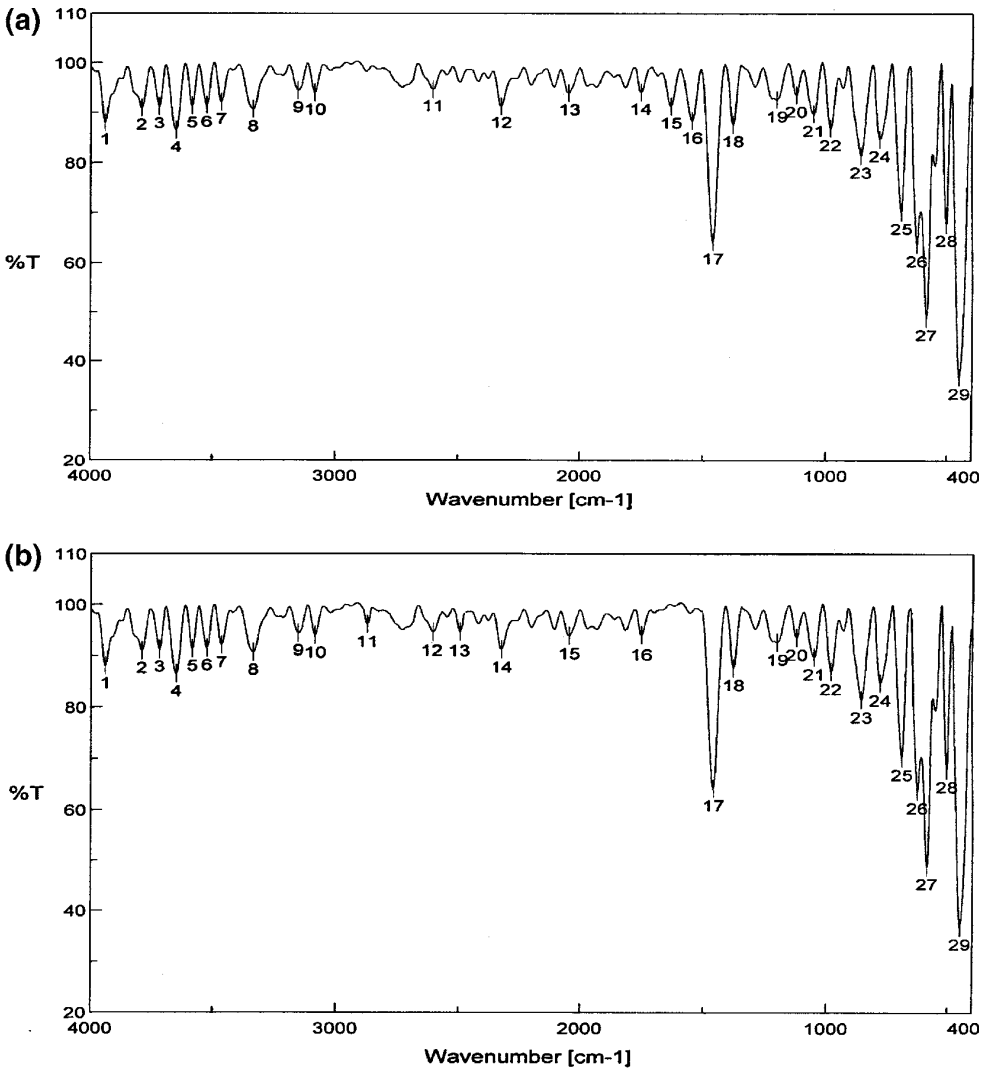

Fig. 8 FTIR spectra of **a** MMN and **b** scratched MS surface adsorbed MMN film

NBT and MBN were found at 1,645, 1,630, 1,643 and 1,587 cm^{-1}, and carbonyl stretching frequencies were observed at 1,726, 1,672, 1,726 and 1,697 cm^{-1}, respectively. In the FTIR spectra of scrapped samples, the stretching frequencies of the azomethine and carbonyl groups were found to be disappeared in the case of PMN, MMN and MBN, but in the case of NBT azomethine group was also disappeared and carbonyl stretching frequency was found to be slightly shifted to lower frequency (1,689 cm^{-1}). These observations confirm that the azomethine and carbonyl groups of PMN, MMN, NBT and MBN are involved in the complex formation with the metal.

Potentiodynamic polarization studies

Polarization measurements were carried out to know the kinetics of anodic and cathodic reactions. Figure 11 reveals the polarization curves for MS in 0.5 M HCl in the absence and presence of different concentrations of PMN, MMN, NBT and MBN at 30 °C. Inspection of Tafel extrapolation plots showed that the addition of inhibitors hindered the acid attack on the MS electrode. In all the cases, the addition of inhibitors reduces both anodic and cathodic current densities indicating that these inhibitors exhibit cathodic and anodic inhibition effects, hence they are relatively mixed type of inhibitors [44, 45].

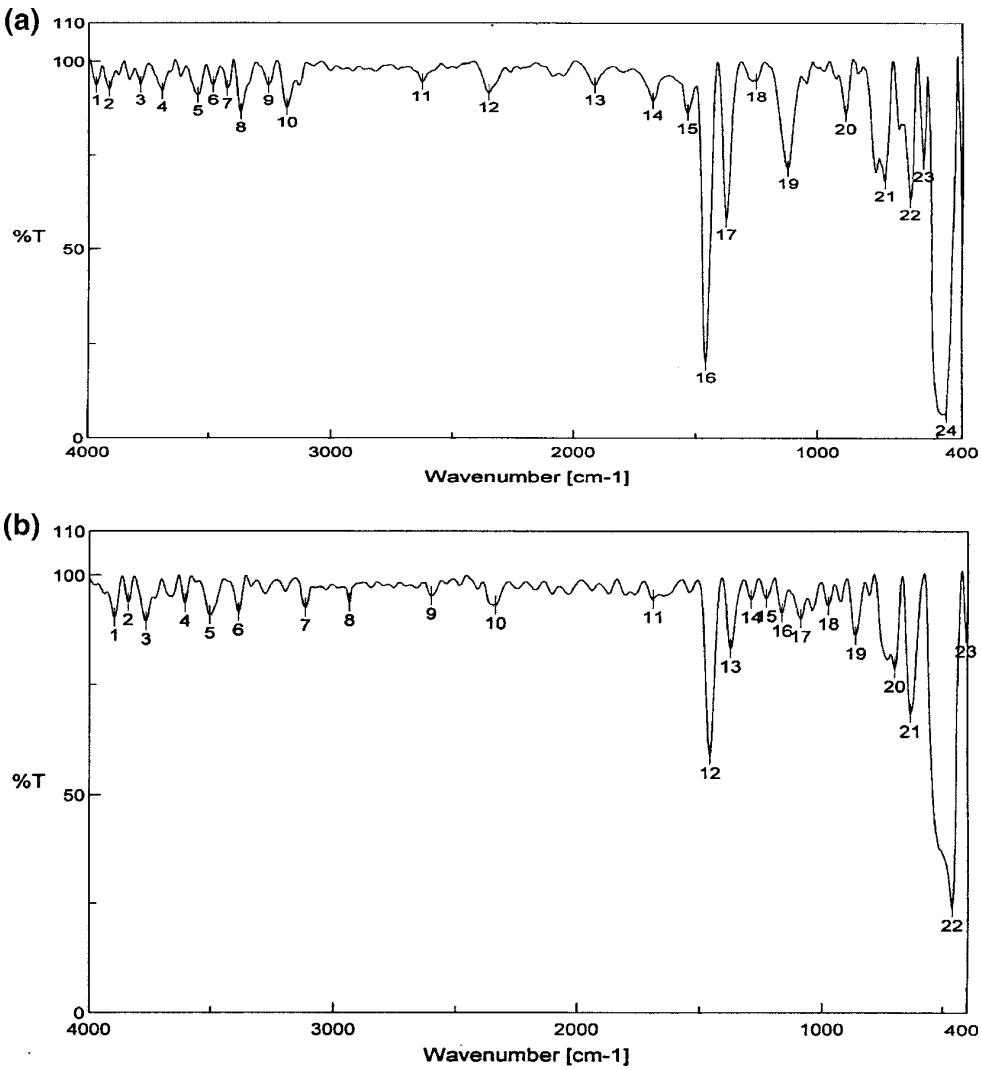

Fig. 9 FTIR spectra of **a** NBT and **b** scratched MS surface adsorbed NBT film

As the corrosion current density decreases, there will be a corresponding decrease in the electron transfer in the redox process; therefore the rate of corrosion reaction becomes slower. Usually a very good corrosion protection can be seen at low current density and at long anodization time due to the diminution of the porosity of the anodic films formed. Table 4 clearly highlights that there is a gradual decrease in the corrosion potential and corrosion current values as the inhibitor concentration was raised from 200 to 500 ppm. The values associated with electrochemical polarization parameters such as corrosion current density (I_{corr}), corrosion potential (E_{corr}), corrosion rate and IE (%) were determined from the polarization plots, and are given in Table 4. The values of corrosion current densities were obtained by extrapolating the current–potential lines to the corresponding corrosion potentials. It is evident that IE (%) increases with inhibitors concentration, and protection action of PMN, MMN, NBT and MBN can be attributed to the electron density of the azomethine (–C=N–) group and this electron density varies with the substituent's in the inhibitor molecules. The imine nitrogen can donate the lone pair of electrons to the metal surface more easily and hence reduces the corrosion rate. The IE (%) was found to be in the order: MBN > NBT > MMN > PMN, which can probably be explained on the basis of additional functional groups and also the nature of the hetero atoms in the inhibitor molecules.

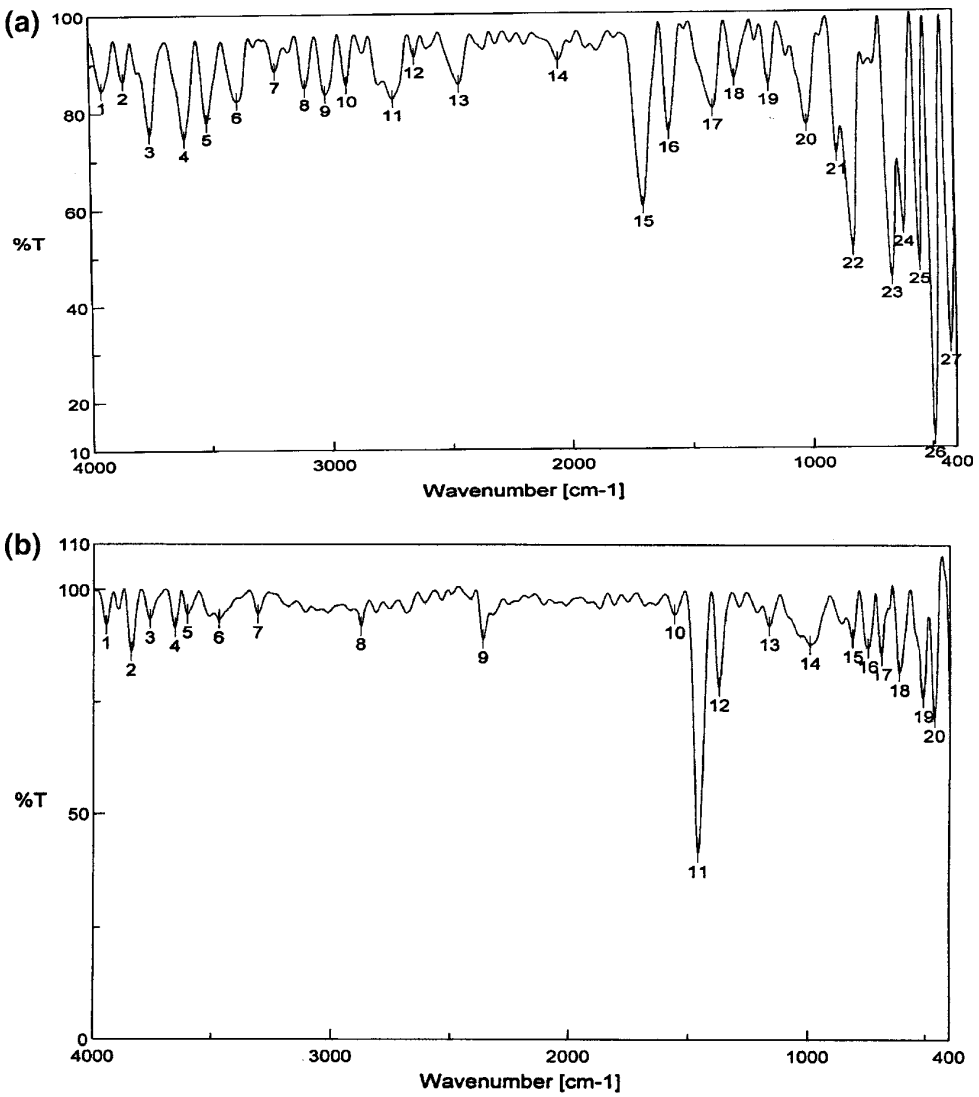

Fig. 10 FTIR spectra of **a** MBN and **b** scratched MS surface adsorbed MBN film

Electrochemical impedance spectroscopy

Nyquist plots for MS in 0.5 M HCl solution with and without different concentrations of PMN, MMN, NBT and MBN are presented in Fig. 12. The Nyquist plots were regarded as one part of the semicircle mostly referred to as frequency dispersion which could be attributed to different physical phenomenon such as roughness, heterogeneities, impurities, grain boundaries and distribution of the surface active sites [46]. The electrochemical impedance parameters derived from the Nyquist plots and IE (%) are listed in Table 5. From the plots, it was clear that the impedance response of MS in uninhibited acid solution has significantly changed after the addition of inhibitors to the corrosive solution. This indicates that the impedance of the inhibited metal has increased with increasing concentration of inhibitors. The measured impedance data were based upon the equivalent circuit, given in the Fig. 13, which consists of constant double layer capacitance (C_{dl}) in parallel with polarization resistance (R_p) which is in series with solution resistance (R_s).

It was observable that, R_p values in the absence of the inhibitors were always lower than those in the presence of the inhibitors. The increase in the R_p values in the presence of different concentrations of PMN, MMN, NBT and MBN indicates reduction in the MS corrosion rate with the

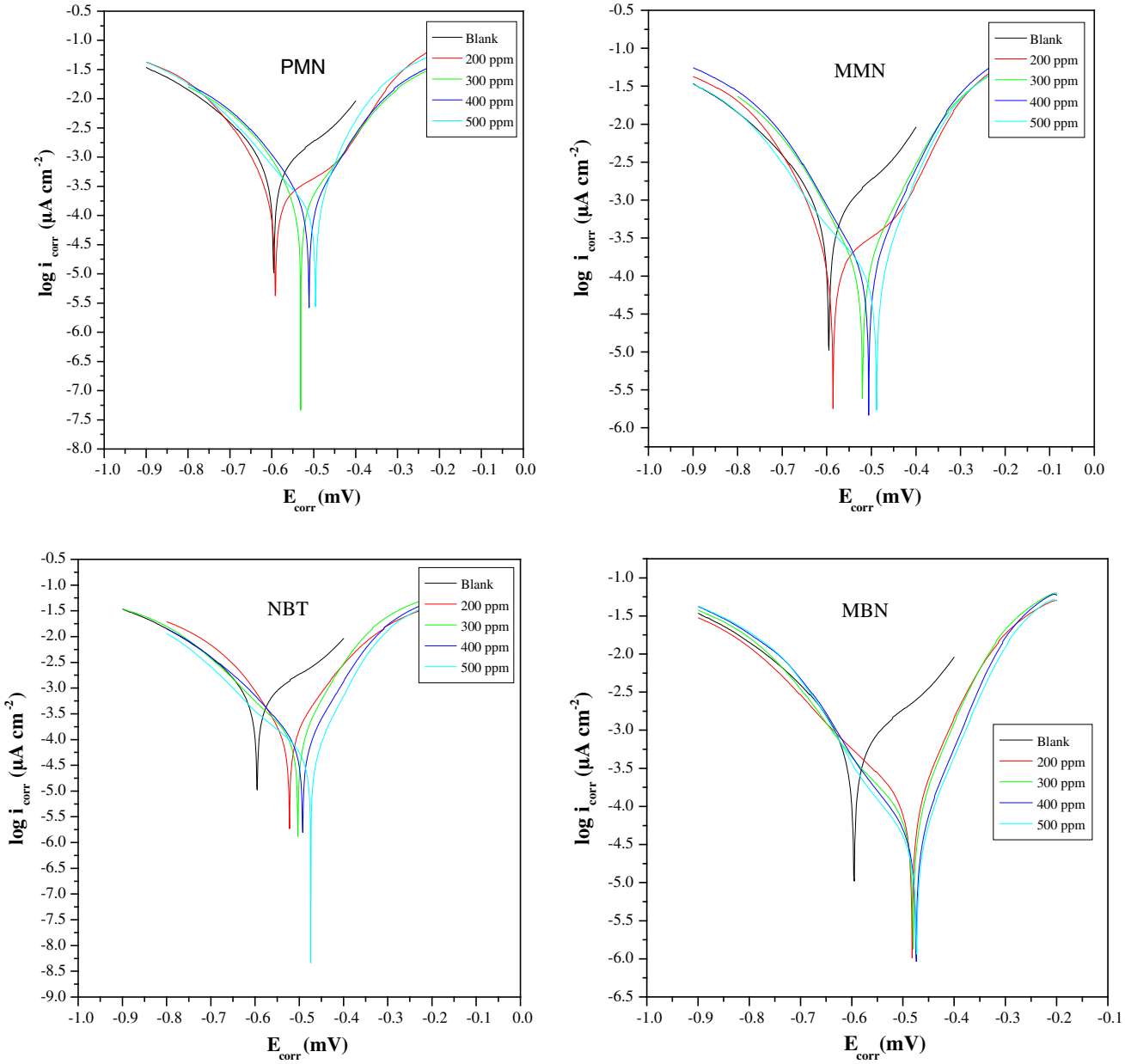

Fig. 11 Polarization curves of MS in 0.5 M HCl in the presence of different concentrations of PMN, MMN, NBT and MBN

formation of adsorbed protective film on the metal-solution interface [47, 48]. When the concentration was raised from 200 to 500 ppm, there was a gradual increase in the diameter of each semicircle of the Nyquist plot reflecting the increase in R_p values from 27.81 to 163.8, 190.5, 316.8 and 562.0 Ω cm^2 for PMN, MMN, NBT and MBN, respectively which indicates the adsorption of inhibitor molecules on the metal surface and also increase in stability of inhibitors film adsorbed on the metal surface.

The double layer capacitance (C_{dl}) values were decreased due to decrease in local dielectric constant and/or an increase in the thickness of the electrical double layer, indicating that the inhibitor molecules adsorbed at the metal-solution interface [49, 50]. Decrease in the surface area [51] and imperfections of the metal surface may also be the reason for decrease of C_{dl} values. Addition of inhibitors provided lower C_{dl} values because of the replacement of water molecules by inhibitor molecules at

Table 4 Polarization parameters and corresponding inhibition efficiency (IE) for the corrosion of the MS in 0.5 M HCl without and with various concentrations of PMN, MMN, NBT and MBN

Inhibitor	C (ppm)	$-E_{corr}$ (mV)	I_{corr} (μA cm^{-2})	IE (%)
Blank	0	0.595	711	–
PMN	200	0.592	224	68.5
	300	0.531	187.1	73.7
	400	0.511	160.5	77.4
	500	0.496	114.9	83.8
MMN	200	0.586	162.4	77.1
	300	0.520	126.4	82.2
	400	0.506	120.6	83.0
	500	0.488	95.26	86.6
NBT	200	0.522	121.2	82.9
	300	0.503	113.6	84.0
	400	0.492	74.15	89.6
	500	0.474	50.5	92.9
MBN	200	0.482	102.3	85.6
	300	0.480	69.42	90.2
	400	0.474	40.18	94.3
	500	0.473	31.84	95.5

the electrode surface [52]. It was clear that as the immersion time increases the R_p values increase and C_{dl} values decrease which indicate the higher protection efficiency as a result of slow adsorption of these inhibitor molecules on to the surface of MS. However, when the immersion time is further enhanced, a sudden decrease in R_p values and increase in C_{dl} values were observed. This behaviour can be due to the instability of the passive film or desorption of the inhibitor molecules.

Mechanism of inhibition

The inhibition effect of nicotinamide derivatives towards the corrosion of MS in 0.5 M HCl solution may be attributed to the adsorption of these compounds at the metal-solution interface. The principal type of interaction between an organic inhibitor and metal surface is physisorption or chemisorption or both. The adsorption of inhibitor is influenced by the nature of the metal, chemical structure of inhibitors, type of aggressive electrolyte, temperature and the morphology of MS [53, 54]. The values of inhibition efficiency depend essentially on the electron density at the active centre of the inhibitor molecule. The thermodynamic parameters showed that the adsorption of these inhibitors on the MS surface in 0.5 M HCl solution involves both chemisorption and physisorption. Chemisorption of these inhibitors arises from the donor–acceptor interactions between the free electron pairs of hetero atoms and π electrons of multiple bonds as well as phenyl group and vacant d orbitals of iron [55].

The inhibition effect of PMN, MMN, NBT and MBN is due to the interaction of π-electrons of pyrrole, pyridine and phenyl rings as well as the presence of electron donor groups such as N, O, S, CH_3 and C=N, through which the inhibitors adsorbed on the MS surface forming insoluble, stable and uniform thin film. Greater corrosion inhibition behaviour of compound MBN is linked to the electron donating effect of thiomethyl group attached to aromatic ring, which increases the electron density on the benzene ring. The increasing delocalization electron density in the molecule may be responsible for inhibiting corrosion process. The adsorption of inhibitor molecules is further stabilized by participation of π-electrons of benzene ring. The good inhibition efficiency of NBT compare to MMN and PMN may be due to the presence of extra thiol (SH) group. MMN (86 %) and PMN (83 %) are structurally almost similar exhibiting comparable corrosion inhibition efficiency at 500 ppm. The order of inhibition efficiency of the four inhibitors from mass loss, potentiodynamic polarization and EIS studies was found to be: MBN > NBT > MMN > PMN.

EDX analysis

EDX spectra were used to determine the elements present on MS surface before and after exposure to the inhibitor solution. The results are displayed in Fig. 14. Figure 14a is the EDX spectrum of polished MS sample and it is notable that the peak of oxygen is absent which confirms the absence of air formed oxide film. However, for inhibited solutions (Fig. 14b–e) the additional lines characteristics for the existence of N, O and S (due to the N and O atoms of the PMN and MMN, N, O and S atoms of the NBT and MBN) in the EDX spectra were obtained. These data showed that the N, O and S atoms of inhibitors are involved in bonding with the MS electrode surface. These results confirm those obtained from IR and SEM observations.

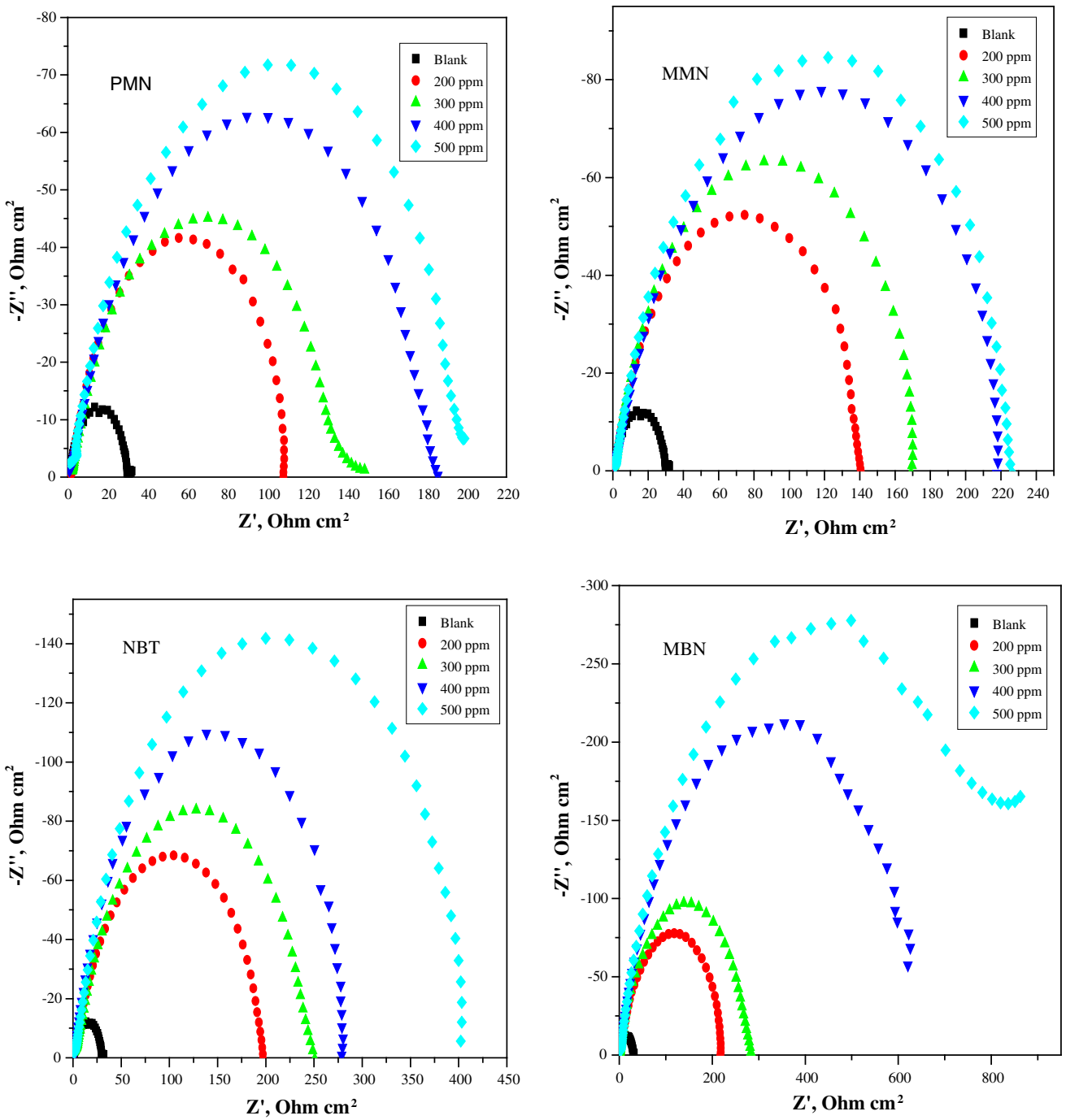

Fig. 12 Nyquist plots for MS in 0.5 M HCl in the presence of different concentrations of PMN, MMN, NBT and MBN

Table 5 Impedance parameters for the corrosion of MS in 0.5 M HCl in the absence and presence of different concentrations of PMN, MMN, NBT and MBN

Inhibitor	C (ppm)	R_P (Ω cm^2)	C_{dl} (μF cm^{-2})	IE (%)
Blank	0	27.8	322.0	–
PMN	200	95.7	91.07	71.0
	300	111.8	81.01	75.1
	400	143.2	80.60	80.6
	500	163.8	64.28	83.0
MMN	200	117.8	80.66	76.4
	300	142.7	72.68	80.5
	400	172.1	65.99	83.8
	500	190.5	61.96	85.4
NBT	200	153.3	76.87	81.8
	300	191.4	66.6	85.5
	400	239.7	56.88	88.4
	500	316.8	51.49	91.2
MBN	200	172.1	65.99	83.8
	300	216.3	60.41	87.1
	400	435.3	48.09	93.6
	500	562.0	36.53	95.1

SEM analysis

The SEM images of the polished and corroded MS surface in the absence and presence of inhibitors are shown in Fig. 15a–f. Figure 15a represents the SEM image for polished MS surface. Figure 15b is the SEM image of MS surface in 0.5 M HCl without inhibitor. It was found that the corroded MS surface contains large number of pits. However, SEM images of MS surface in the presence of inhibitors (Fig. 15c–f) were observed to be smoother than that of MS surface in 0.5 M HCl alone. These observations reveal that the inhibitors form protective layer on the MS surface, which prevents the attack of acid as well as the dissolution of MS by forming surface adsorbed layer and thereby reducing the corrosion rate.

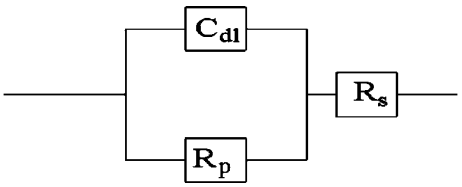

Fig. 13 Equivalent circuit used to fit the impedance spectra

Conclusion

1. All the synthesized nicotinamide derivatives showed good inhibition efficiency for the corrosion of MS in 0.5 M HCl solutions and the inhibition efficiency found to be time, temperature and concentration dependent.
2. Langmuir adsorption isotherm was found to be the best description for the studied inhibitors, and the negative values of Gibbs free energy of adsorption indicate that the adsorption of inhibitors involves both physisorption and chemisorption process.
3. The inhibition efficiency was found in the order: MBN > NBT > MMN > PMN and the inhibition efficiencies determined by mass loss, potentiodynamic polarization and EIS methods are in good agreement with each other.

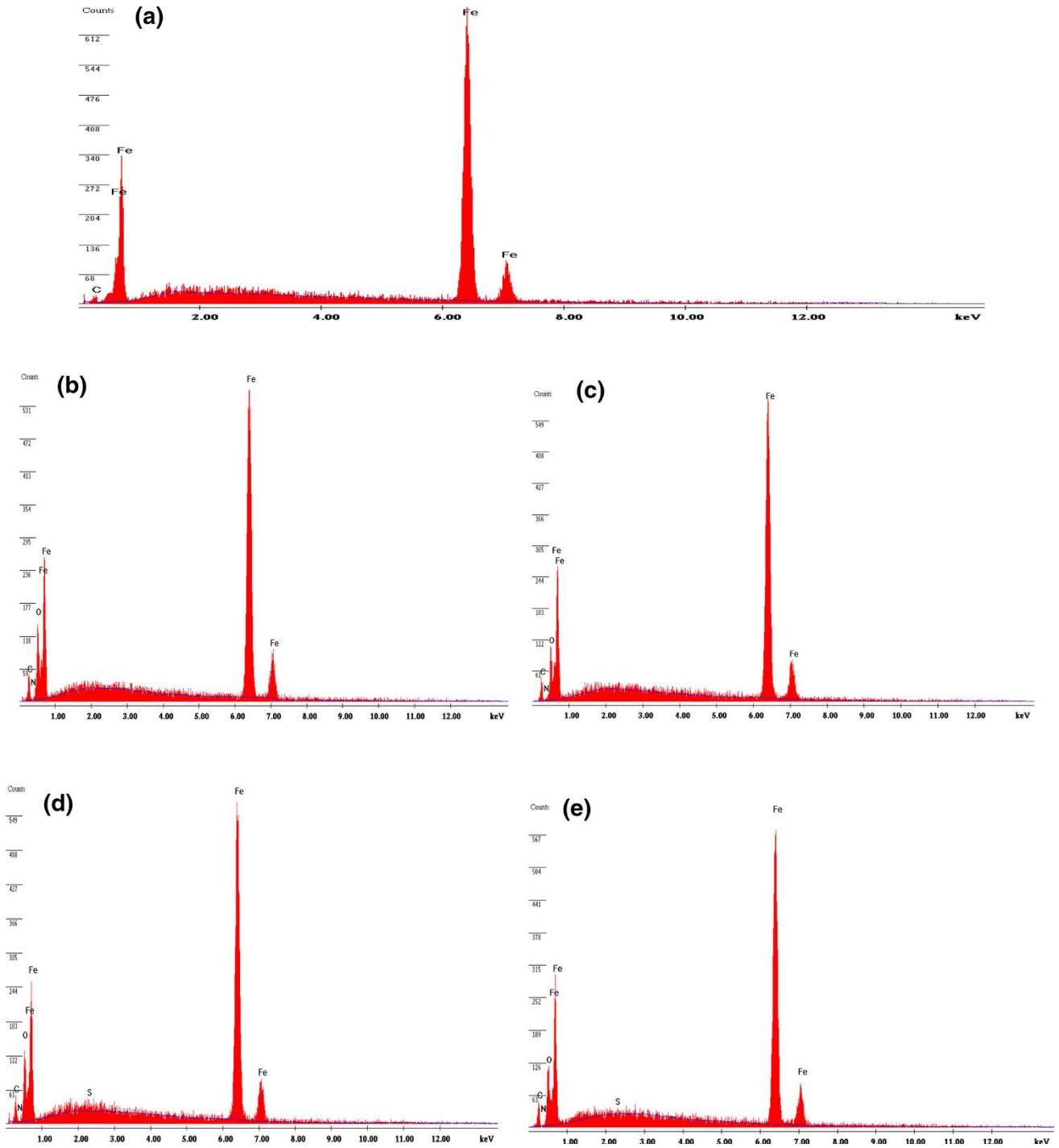

Fig. 14 EDX images of **a** polished MS surface, **b** MS in 500 ppm PMN, **c** MS in 500 ppm MMN, **d** MS in 500 ppm NBT and **e** MS in 500 ppm MMN

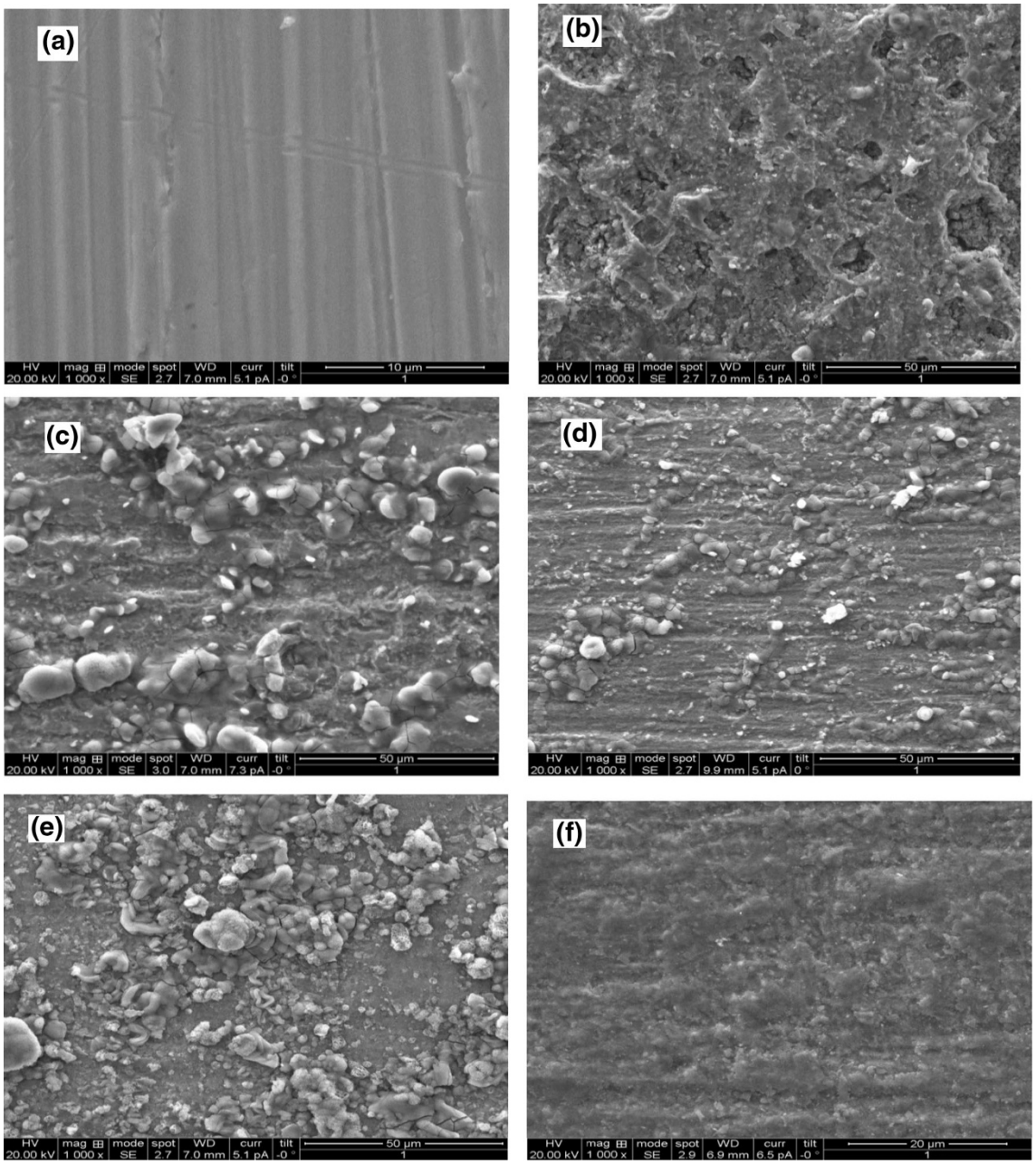

Fig. 15 SEM images of **a** polished MS surface, **b** MS in 0.5 M HCl, **c** MS in 500 ppm PMN, **d** MS in 500 ppm MMN, **e** MS in 500 ppm NBT and **f** MS in 500 ppm MBN

4. FTIR spectra, scanning electron microscopy (SEM) and energy dispersive X-ray spectroscopy (EDX) were performed to characterize the passive film on the metal surface.

Author's contribution KNM: Writing paper, Guidance. MPC: testing in laboratory. CBP: making set up. All authors read and approved the final manuscript.

Acknowledgments One of the authors (MPC) is grateful to University of Mysore, Mysore for awarding SRF to carry out the research work.

Conflict of interest The authors declare that they have no competing interests.

References

1. Nathan NN (1997) Corrosion inhibitors. National association of corrosion engineerings, Houston
2. Trabanelli G (1991) Inhibitors. An old remedy for new challenge. Corros 47:410–419
3. Arena MA, Conde A, De Damborenea J (2002) Cerium: a suitable green corrosion inhibitor for tinplate. Corros Sci 44:511–520
4. Cano E, Pinila P, Pole JL, Bastidas JM (2003) Copper corrosion inhibition by fast green, fuchsin acid and basic compounds in citric acid solution. Mater Corros 54:222–228
5. Dong-Jin C, Youg-Wook K, Jung-Gu K (2001) Development of a blended corrosion, scale, and microorganism inhibitor for open recirculating cooling systems. Mater Corros 52:697–704
6. Moretti G, Guidi F, Grion G (2004) Tryptamine as a green iron corrosion inhibitor in 0.5 M deaerated sulphuric acid. Corros Sci 46:387–403
7. Abd El-Maksoud SA (2008) The effect of organic compounds on the electrochemical behaviour of steel in acidic media. A review. Int J Electrochem Sci 3:528–555
8. Quraishi MA, Sardar R (2003) Corrosion inhibition of mild steel in acid solutions by some aromatic oxadiazoles. Mater Chem Phys 78:425–431
9. Sachin MS, Bilgic S, Yilmaz H (2002) The inhibition effects of some cyclic nitrogen compounds on the corrosion of the steel in NaCl mediums. Appl Surf Sci 195:1–7
10. Abdulla M, Al-Agez M, Fouda AS (2009) Phenylhydrazone derivatives as corrosion inhibitors for-α-brass in hydrochloric acid solutions. Int J Electrochem Sci 4:336–352
11. Bouklah M, Aouniti A, Hammouti B, Benkaddour M, Lagrenee M, Bentiss F (2004) Effect of the substitution of an oxygen atom by sulphur in a pyridazinic molecule towards inhibition of corrosion of steel in 0.5 M H_2SO_4 medium. Prog Org Coatings 51:118–124
12. Bentiss F, Traisnel M, Vezin H, Hildebrand HF, Lagrenee M (2004) 2,5-Bis(4-dimethylaminophenyl)-1,3,4-oxadiazole and 2,5-bis(4-dimethylaminophenyl)-1,3,4-thiadiazole as corrosion inhibitors for mild steel in acidic media. Corros Sci 46:2781–2792
13. Wang H, Liu R, Xin J (2004) Inhibiting effects of some mercapto-triazole derivatives on the corrosion of mild steel in 1.0 M HCl medium. Corros Sci 46:2455–2466
14. Karakus M, Sahin M, Bilgic S (2005) An investigation on the inhibition effects of some new dithiophosphonic acid monoesthers on the corrosion of the steel in 1 M HCl medium. Mater Chem Phys 92:565–571
15. Afidah A, Rahim E, Rocca J, Steinmetz MJ, Kassim RA, Sani Ibrahim M (2007) Mangrove tannins and their flavanoid monomers as alternative steel corrosion inhibitors in acidic medium. Corros Sci 49:402–417
16. Li W, He Q, Pei C, Hou B (2007) Experimental and theoretical investigation of the adsorption behaviour of new triazole derivatives as inhibitors for mild steel corrosion in acid media. Electrochim Acta 52:6386–6394
17. Wang L (2006) Inhibition of mild steel corrosion in phosphoric acid solution by triazole derivatives. Corros Sci 48:608–616
18. Nataraja SE, Venkatesha TV, Manjunath K, Poojary Boja, Pavithra MK, Tandon HC (2011) Inhibition of the corrosion of steel in hydrochloric acid solution by some organic molecules containing the methylthiophenyl moiety. Corros Sci 53:2651–2659
19. Negm NA, Ghuiba FM, Tawfik SM (2011) Novel isoxazolium cationic Schiff base compounds as corrosion inhibitors for carbon steel in hydrochloric acid. Corros Sci 53:3566–3575
20. Ebenso EE, Obot IB, Murulana LC (2010) Quinoline and its derivatives as effective corrosion inhibitors for mild steel in acidic medium. Int J Electrochem Sci 5:1574–1586
21. Ebenso EE, Arslan T, Kandemirli F, Love I, Ogretir C, Saracoglu M, Umoren SA (2010) Theoretical studies of some sulphonamides as corrosion inhibitors for mild steel in acidic medium. Int J Quan Chem 110:2614–2636
22. Loto RT, Loto CA, Popoola API (2012) Corrosion inhibition of thiourea and thiadiazole derivatives: a review. J Mater Environ Sci 3:885–894
23. Bereket G, Hur E, Ogretir C (2002) Quantum chemical studies on some imidazole derivatives as corrosion inhibitors for iron in acidic medium. J Mol Stru (Theochem) 578:79–88
24. Acharya S, Upadhyay SN (2004) The inhibition of corrosion of mild steel by some fluoroquinolones in sodium chloride solution. Trans Indian Inst Met 57:297–306
25. Herrag L, Chetouani A, Elkadiri S, Hammouti B, Aouniti A (2008) Pyrazole derivatives as corrosion inhibitors for steel in hydrochloric acid. Portugal Electrochim Acta 26:211–220
26. Zerga B, Hammouti B, Ebn Touhami M, Touir R, Taleb M, Sfaira M, Bennajeh M, Forssal I (2012) Comparative inhibition study of new synthesized pyridazine derivatives towards mild steel corrosion in hydrochloric acid. Part-II: Thermodynamic proprieties. Int J Electrochem Sci 7:471–483
27. Elewady GY (2008) Pyrimidine derivatives as corrosion inhibitors for carbon steel in 2M hydrochloric acid solution. Int J Electrochem Sci 3:1149–1161
28. Praveen Kumar P, Rani BL (2011) Synthesis and characterization of new Schiff bases containing pyridine moiety and their derivatives as antioxidant agents. Int J Chem Tech Res 3:155–160
29. Bentiss F, Lagrenee M, Traisnel M, Hornez JC (1999) The corrosion inhibition of mild steel in acidic media by a new triazole derivative. Corros Sci 41:789–803
30. Singh A, Singh AK, Quraishi MA (2010) Dapsone: a novel corrosion inhibitor for mild steel in acid media. Open Electrochem J 2:43–51
31. Quraishi MA, Hariom K (2002) Sharma, 4-Amino-3-butyl-5-mercapto-1,2,4-triazole: a new corrosion inhibitor for mild steel in sulphuric acid. Mater Chem Phys 78:18–21
32. Poornima T, Nayak J, Shetty AN (2012) Corrosion inhibition of the annealed 18Ni 250 grade maraging steel in 0.67 M phosphoric acid by 3,4- dimethoxybenzaldehydethiosemicarbazone. Chem Sci J 69:1–13
33. Abdallah M, Heal EA, Fouda AS (2006) Aminopyrimidine derivatives as inhibitors for corrosion of 1018 carbon steel in nitric acid solution. Corros Sci 48:1639–1654
34. Abd El Rehim SS, Rafaey SAM, Taha F, Saleh MB, Ahmed RA (2001) Corrosion inhibition of mild steel in acidic medium using 2-amino thiophenol and 2-cyanomethyl benzothiazole. J Appl Electrochem 31:429–435
35. Yurt A, Balaban A, Kandemir SU, Bereket G, Erk B (2004) Investigation on some Schiff bases as HCl corrosion inhibitors for carbon steel. Mater Chem Phys 85:420–426
36. Tang L, Li X, Si Y, Mu G, Liu G (2006) The synergistic inhibition between 8- hydroxyquinoline and chloride ion for the corrosion of cold rolled steel in 0.5M sulfuric acid. Mater Chem Phys 95:29–38
37. Bhattacharya AK, Naiya TK, Mandal SN, Das SK (2008) Adsorption, kinetics and equilibrium studies on removal of Cr(VI) from aqueous solutions using different low-cost adsorbents. Chem Engg J 137:529–541
38. Refaey SAM, Taha F, Abd El-Malak AM (2006) Corrosion and inhibition of 316L stainless steel in neutral medium by 2- mercaptobenzimidazole. Int J Electrochem Sci 1:80–91

39. Li X, Deng S, Fu H (2011) Three pyrazine derivatives as corrosion inhibitors for steel in 1.0 M H_2SO_4 solution. Corros Sci 53:3241–3247
40. Bouklah M, Hammouti B, Lagrenee M, Bentiss F (2006) New thio-compounds as corrosion inhibitor for steel in 1 M HCl. Corros Sci 48:2470–2479
41. Bayoumi FM, Ghanem WA (2005) Corrosion inhibition of mild steel using naphthalene disulfonic acid. Mater Letts 59: 3806–3809
42. Yurt A, Balaban A, Ustun Kandemir S, Bereket G, Erk B (2004) Investigation on some Schiff bases as HCl corrosion inhibitors for carbon steel. Mater Chem Phys 85:420–426
43. Li X, Deng S, Fu H, Li T (2009) Adsorption and inhibition effect of 6-benzylaminopurine on cold rolled steel in 1.0 M HCl. Electrochim Acta 54:4089–4098
44. Lebrini M, Bentiss F, Vezin H, Lagrenee M (2005) Inhibiting effects of some oxadiazole derivatives on the corrosion of mild steel in perchloric acid solution. Appl Surf Sci 252:950–958
45. Musa AY, Kadhum AAH, Mohamad AB, Takriff MS, Daud AR, Kamarudin SK (2010) On the inhibition of mild steel corrosion by 4-amino-5-phenyl-4H-1,2,4-trizole-3-thiol. Corros Sci 52: 526–533
46. Juttner K (1990) Electrochemical impedance spectroscopy (EIS) of corrosion processes on inhomogeneous surfaces. Electrochim Acta 35:1501–1508
47. Bentiss F, Lebrini M, Langrenee M, Traisnel M, Elfarouk A, Vezin H (2007) The influence of some new 2,5-disubstituted 1,3,4-thiadiazoles on the corrosion behaviour of mild steel in 1 M HCl solution: AC impedance study and theoretical approach. Electrochim Acta 52:6865–6872
48. El-Taib Heakal F, Ghoneim AA, Fekry AM (2007) Stability of spontaneous passive films on high strength Mo-containing stainless steels in aqueous solutions. J Appl Electrochem 37: 405–413
49. Lebrini M, Bentiss F, Vezin H, Lagrene M (2006) The inhibition of mild steel corrosion in acidic solutions by 2,5-bis(4-pyridyl)-1,3,4-thiadiazole: structure–activity correlation. Corros Sci 48:1279–1291
50. Shukla SK, Quaraishi MA (2010) The effects of pharmaceutically active compound doxycycline on the corrosion of mild steel in hydrochloric acid solution. Corros Sci 52:314–321
51. Bentiss F, Traisnel M, Lagrenee M (2000) The substituted 1,3,4-oxadiazoles: a new class of corrosion inhibitors of mild steel in acidic media. Corros Sci 42:127–146
52. Parameswari K, Chaitra S, Nusrath Unnisa C, Selvaraj A (2010) Effect of azlactones on corrosion inhibition of mild steel in acid medium. J Appl Sci Res 6:1100–1110
53. Aloui S, Forsal I, Sfaira M, Ebn Touhami M, Taleb M, Filali Baba M, Daoudi M (2009) New mechanism synthesis of 1,4-benzothiazine and its inhibition performance on mild steel in hydrochloric acid. Portugaliae Electrochim Acta 27:599–613
54. Zaafarany I (2009) Phenyl phthalimide as corrosion inhibitor for corrosion of C-Steel in sulphuric acid solution. Portugaliae Electrochim Acta 27:631–643
55. Ahamad I, Quraishi MA (2009) Bis (benzimidazol-2-yl) disulphide: an efficient water soluble inhibitor for corrosion of mild steel in acid media. Corros Sci 51:2006–2013